

# Theoretical study of the bifunctional-urea catalyzed Michael reaction of 1,3-dicarbonyl compounds and nitroolefins: reaction mechanism and enantioselectivity

Rongxiu Zhu, Dongju Zhang, Jian Wu and Chengbu Liu\*

*School of Chemistry and Chemical Engineering, Shandong University, Jinan 250100, PR China*

Received 3 April 2006; accepted 24 May 2006

**Abstract**—The Michael reaction of nitroalkenes catalyzed by a bifunctional-urea is studied using density functional theory (DFT) calculations, to determine the detailed catalytic mechanism and key factors controlling the enantioselectivity. Four reaction channels, corresponding to the different approach modes of nitroalkenes to a chiral scaffold and different processes of second proton transfer, have been characterized. The rate determining step is proton transfer from the amino group of a catalyst to an  $\alpha$ -carbon of nitronate, and the enantioselectivity is controlled by the steps involved in carbon–carbon bond formation. The calculated results provide a general model that explains the mechanism and enantioselectivity of the title reaction.

© 2006 Elsevier Ltd. All rights reserved.

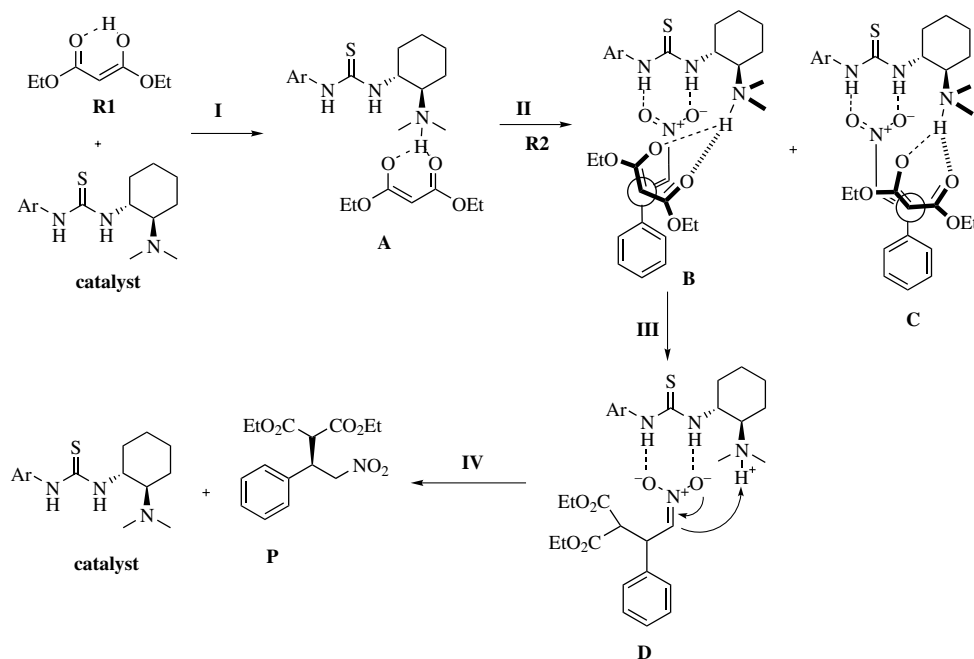
## 1. Introduction

Asymmetric organocatalysis, in which the reaction is mediated by a catalytic amount of a chiral organic molecule, is becoming a powerful tool in organic synthesis.<sup>1–3</sup> A number of asymmetric organocatalytic reactions have recently been developed, and new asymmetric reactions are constantly being reported.<sup>4–7</sup> Current studies in this area have focused on the development of new enantioselective catalysts with high activity and broad generality. Bifunctional urea derivatives, with both a urea or thiourea moiety and a tertiary amino group on a chiral scaffold, would be able to activate both electrophilic and nucleophilic substrates at the positions defined by the two functional groups of the catalyst. Hence, urea derivatives have been expected to be efficient catalysts for asymmetric organocatalytic reactions. Recently, while a lot of effort has been made to realize the reactions catalyzed by bifunctional urea derivatives,<sup>8,9</sup> not many theoretical analyses on these important reactions were carried out to clarify the detailed mechanism.<sup>10</sup>

The Michael addition of nitroolefins is one of the most important reactions in organic chemistry due to the enormous versatility of the nitro group and the high reactivity

of nitroalkenes. Though catalytic asymmetric versions of this reaction have been achieved, most require metal catalysts or strict conditions.<sup>11</sup> Recently, L-proline derivatives have been reported to afford Michael adducts with good yields and moderate enantioselectivities.<sup>12</sup> More recently, Takemoto et al.<sup>8</sup> reported the bifunctional-urea catalyzed Michael reactions of 1,3-dicarbonyl compounds to nitroalkenes with high enantioselectivity. They proposed a possible mechanism, as shown in **Scheme 1**, where four steps proceeded in turn: (i) the amino group of the catalyst first deprotonates a proton from the six-membered cyclic enol form of malonate **R1**, to form a binary complex **A**; (ii) **A** interacts with nitroolefin **R2** via hydrogen bonding to give a new ternary complex which is either **B** or **C**; (iii) on the basis of the product configuration, the reaction would proceed through complex **B** to give the nitrate complex **D**, bearing an (*R*)-configuration, with high selectivity; and (iv) the proton migrates from the amino group to nitronate carbon to give product **P** along with the catalyst. It was found that the tertiary amine functionality of the catalyst has a significant effect on the reaction rate, but only a slight effect on the enantioselectivity. However, the role of the amino group played in the reaction is not well understood. In addition, the origin of enantioselectivity of the catalyzed Michael reaction is also unclear. So, intensive theoretical research on this reaction is highly desirable and worthy pursuing.

\* Corresponding author. E-mail: [cbliu@sdu.edu.cn](mailto:cbliu@sdu.edu.cn)



**Scheme 1.** Proposed mechanism for the reaction of malonate and nitroolefins.<sup>8</sup>

Herein, we report the reaction of malonate with nitroolefins catalyzed by a bifunctional-urea catalyst as a prototype of catalyzed Michael reactions for study and perform detailed density functional theory (DFT) calculations on it. Our aims are to (a) shed light on the mechanistic details of this catalyzed reaction and hence obtain a better interplay between theory and experiment, (b) understand the roles of the bifunctional groups of the catalyst and the origin of enantioselectivity for the catalyzed Michael reaction of malonate with nitroolefins, and (c) provide a general profile of the Michael reaction catalyzed by bifunctional-urea catalysts.

## 2. Models and computational details

The bifunctional-urea catalyst was modeled by a simple molecule (denoted as **cat.**) that involves the essential structural features of the catalyst (see **Scheme 2**). Geometry optimizations were carried out using the B3LYP functional<sup>13</sup> with the 6-31G basis set for all atoms.<sup>14</sup> Polarization functions were added for the atoms directly involved in bond-forming and bond-breaking processes [N ( $\zeta_d = 0.864$ ), C ( $\zeta_d = 0.600$ ), O ( $\zeta_d = 1.154$ ), and H ( $\zeta_p = 1.100$ )]. All relevant stationary points on the potential energy surface (PES) have been located and their nature (local minima or first-order saddle points) characterized by performing vibrational frequency calculations. The intrinsic reaction coordinate (IRC) pathways from the transition states (TSs) to two local minima have been traced in order to verify that each saddle point links the two desired minima. All calculations were carried out with the Gaussian 03 software package.<sup>15</sup> For all cited energies, the zero-point energy (ZPE) corrections have been included.

## 3. Results and discussion

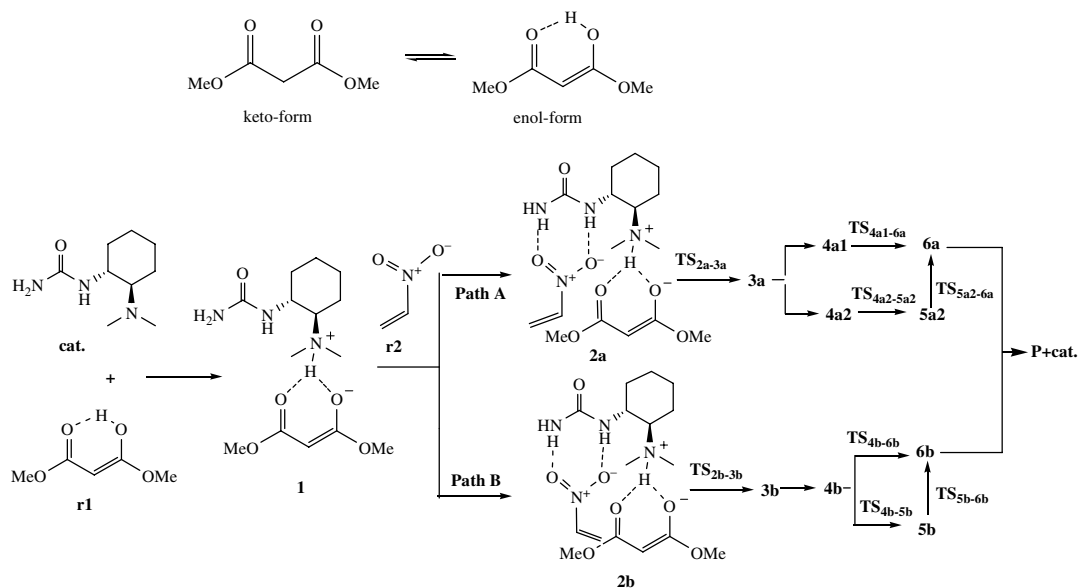
### 3.1. Reaction mechanism

In order to establish the mechanism of the catalyzed Michael reaction, the reaction of dimethyl malonate, denoted as **r1**, with nitroethylene, denoted as **r2**, was studied in detail (see **Scheme 2**).

**r1** can exist as two tautomeric forms in equilibrium, that is, enol-keto tautomerism (see **Scheme 2**). The six-membered cyclic enol form possesses a nucleophilic carbon atom, which can add to active nitroolefins. Thus the enol form was assumed for the catalyzed Michael reaction.

The first step involves the amino group of catalyst removing a proton from the enol form of **r1**, to give the reactive enolate **1**. This process is calculated to be exothermic by  $29.9 \text{ kcal mol}^{-1}$  compared to the reactants (**r1** + **cat.**), indicating that the proton migration is an energetically favorable process.

The nitroethylene **r2** then interacts with **1** through two O...HN hydrogen bonds. There are two possible pathways, denoted as pathways **A** and **B**, for the reaction of **r2** and **1** to yield the product and catalyst, which differ in the approach mode of the reactants (see **2a**, **2b**, and **TS**<sub>2a-3a</sub>, **TS**<sub>2b-3b</sub> in **Fig. 1**). In **2a** and **TS**<sub>2a-3a</sub>, the carbon-carbon double bond of the nitroethylene points away from the chiral scaffold, while in **2b** and **TS**<sub>2b-3b</sub>, the  $\alpha$ -hydrogen of nitroethylene points away from the chiral scaffold. The structures of the intermediates and TSs involved in these two pathways have been located and shown in **Figure 1**, and the calculated energetic profiles along the two pathways are given in **Figure 2**.



**Scheme 2.** Mechanism details for the reaction of dimethyl malonate and nitroethylene with the urea derivative, proposed from the present calculations.

In pathway **A**, **r2** interacts with **1** through two weak  $\text{NH}\cdots\text{O}$  hydrogen bonds of 2.064 and 2.214 Å, forming a new complex **2a**, lying  $8.91\text{ kcal mol}^{-1}$  lower in energy than the reactants (**1** + **cat.**). Once **2a** is formed, the nucleophilic addition of the enolate and nitroethylene occurs, giving an adduct, which further interacts with the catalyst via three  $\text{NH}\cdots\text{O}$  hydrogen bonds, to generate intermediate **3a**. This step proceeds via transition state  $\text{TS}_{2a-3a}$ , with a very low barrier of  $4.29\text{ kcal mol}^{-1}$ , lying  $5.26\text{ kcal mol}^{-1}$  lower in energy than **2a**. Finally, the proton migrates from N atom of the amino group of catalyst to carbon C1 atom of the adduct and completes the catalytic cycle.

The second proton migration requires further comment. We found that there are two possible channels, marked as channels  $\text{I}_A$  and  $\text{II}_A$  in Figure 2, for achieving the proton transfer from the amino group to the nitronate carbon. Channel  $\text{I}_A$  is a direct migration process. However, the transferring proton and the C1 carbon atom in **3a** are too far away to realize the proton delivery, so **3a** must distort its geometry to **4a1**, to allow proton and C1 to reach a proper distance, without raising its energy too much. **4a1** is calculated only to be  $0.69\text{ kcal mol}^{-1}$  higher in energy than **3a**. Then the proton migrates via saddle point  $\text{TS}_{4a1-6a}$  with a barrier of  $5.58\text{ kcal mol}^{-1}$ . This channel is exothermic by  $11.16\text{ kcal mol}^{-1}$  compared to **4a1**. Complete proton transfer yields the hydrogen-bonded complex **6a**. As the hydrogen bonds between the Michael addition product and catalyst in **6a** break, product **P** along with the catalyst is formed, endothermic by  $10.01\text{ kcal mol}^{-1}$ . The second reaction channel from **3a** (channel  $\text{II}_A$ ) involves an enol-keto tautomerism. Initially, the hydrogen-bonding ( $\text{NH}\cdots\text{O1}$ ) complex **3a** converted into another hydrogen-bonding ( $\text{NH}\cdots\text{O2}$ ) complex **4a2** (see Fig. 1, **3a** and **4a2**), and **4a2** is  $5.20\text{ kcal mol}^{-1}$  more stable compared to **4a1**. Proton transfer from the amino group to O2 of nitro group forms the enol tautomer **5a2** via  $\text{TS}_{4a2-5a2}$ . Finally, **5a2** tautomerizes to keto tautomer **6a** via  $\text{TS}_{5a2-6a}$  to finish the pro-

ton transfer from the amino group to nitronate carbon. The computed results indicate that the relative energy of  $\text{TS}_{4a2-5a2}$  is even below **4a2** and **5a2** after ZPE corrections, indicating the PES at this area is very flat. However, the enol-keto tautomerism of **5a2** to **6a** has a high barrier of  $58.00\text{ kcal mol}^{-1}$ . Therefore, channel  $\text{II}_A$  is energetically less favorable than channel  $\text{I}_A$ .

Pathway **B** has some similarity to pathway **A** since no major steric interactions are present in the reaction. A comparison of the calculated energy profiles for pathways **A** and **B** (Fig. 2) provides further insight into the mechanism. The energy of  $\text{TS}_{2b-3b}$  is only  $0.87\text{ kcal mol}^{-1}$  higher than that of  $\text{TS}_{2a-3a}$ . However, the proton transfer from the amino group to nitronate carbon in **3b** is much less favorable than in **3a**. This can be contributed to three less favorable factors in **3b** than in **3a** (see **3a** and **3b**, and  $\text{TS}_{4a1-6a}$  and  $\text{TS}_{4b-6b}$  in Fig. 1): the longer distance between the transferring proton and nitronate carbon, the stronger steric repulsion interactions between the amino group and malonate group, and a larger geometry change is required (in **3a** and  $\text{TS}_{4a1-6a}$ , the dihedral angle C1–C2–C3–C4 is  $75.6^\circ$  and  $74.3^\circ$ , respectively, the difference being  $1.3^\circ$ ; while in **3b** and  $\text{TS}_{4b-6b}$ , the dihedral angle C1–C2–C3–C4 is  $48.3^\circ$  and  $-54.2^\circ$ , respectively, the change is  $102.5^\circ$ ). Instead of distorting the geometry, **3b** converted into another more stable complex **4b**, and **4b** is  $5.20\text{ kcal mol}^{-1}$  more stable than **3b**. Subsequently, the proton transfers from the amino group to nitronate carbon via saddle point  $\text{TS}_{4b-6b}$ , to give the new intermediate **6b**. In the process of proton transfer, the barrier is  $13.12\text{ kcal mol}^{-1}$ , which is  $7.54\text{ kcal mol}^{-1}$  higher than that of channel  $\text{I}_A$ . In comparison with channel  $\text{II}_A$ , **4b** can also be converted into the enol tautomer **5b** with a very flat saddle point  $\text{TS}_{4b-5b}$ , then **5b** tautomerizes to keto tautomer **6b** via  $\text{TS}_{5b-6b}$  with a very high barrier ( $59.94\text{ kcal mol}^{-1}$ ) to finish the proton transfer from the amino group to nitronate carbon. Finally, the hydrogen bonds in **6b** break to form product **P** along with catalyst.

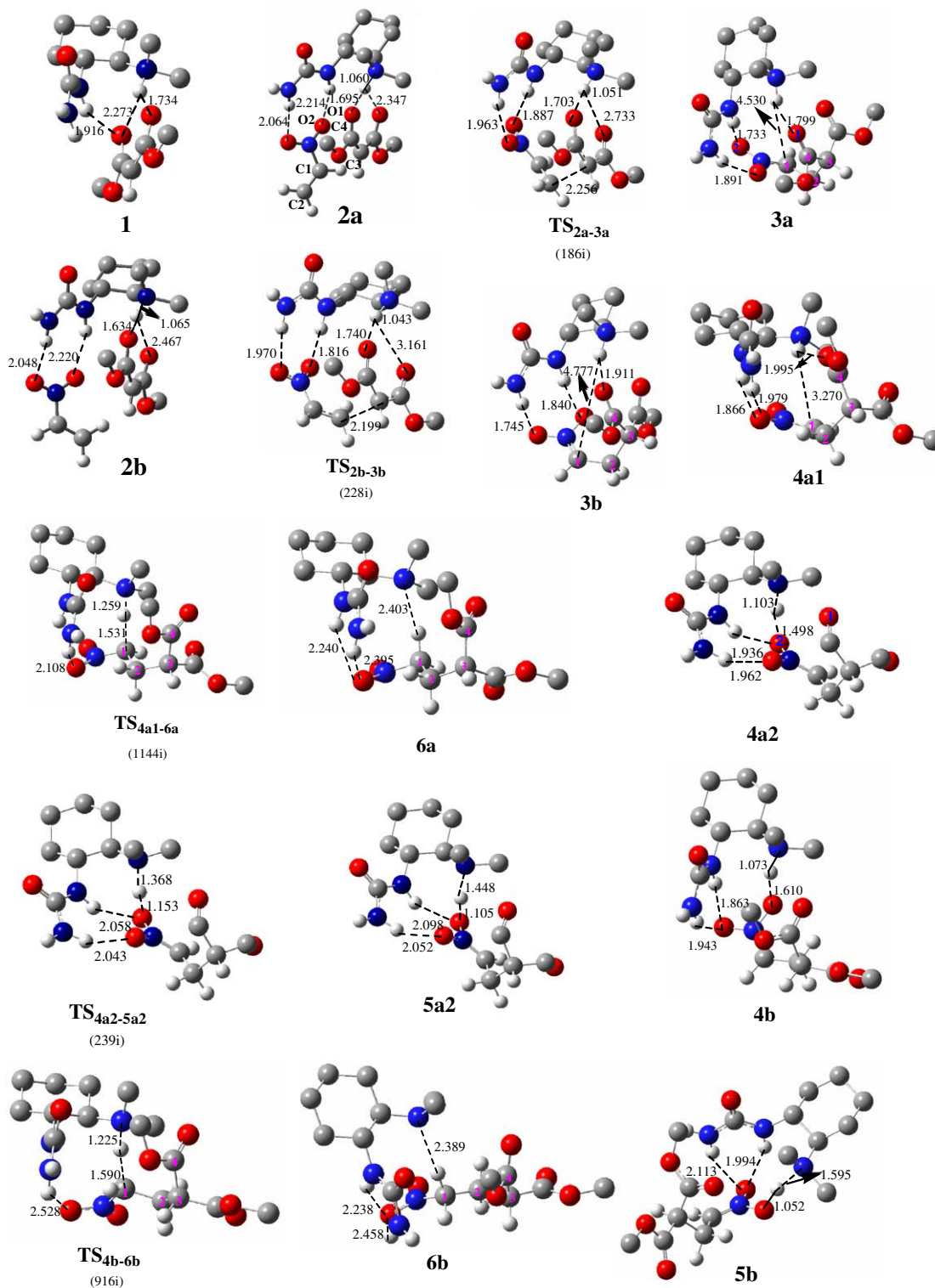


**Figure 1.** Optimized geometries for the intermediates and saddle points involved in the reaction of nitroethylene and malonate (distances in Å). The values in the parentheses refer to the imaginary vibrational frequency corresponding to the transition states. The hydrogen atoms on the rings and methyl groups are omitted for clarity.

Our calculations indicate that channel I<sub>A</sub> for the catalytic Michael reaction between nitroethylene and malonate is energetically more favorable.

Moreover, the basis set superposition errors (BSSEs) corrections for the initial and final steps of the main channels are estimated using the counterpoise method.<sup>16</sup>

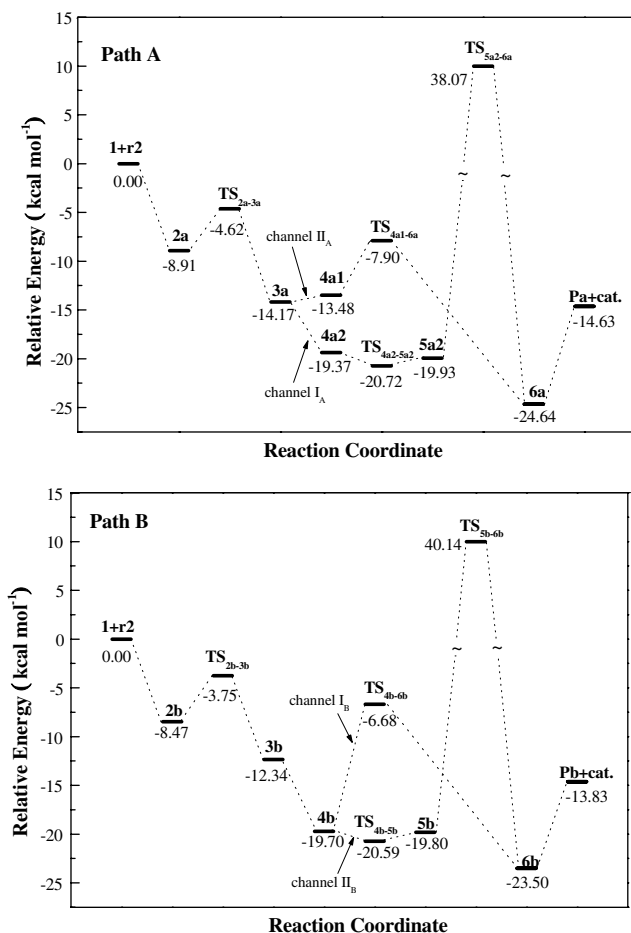


**Figure 2.** Calculated energetic profile for the reaction of nitroethylene and malonate along the reaction coordinate.

The calculated results show that the BSSEs corrections are less than 5.0 kcal mol<sup>-1</sup>, which mainly affect the relative stabilities of the intermediates in the initial and final steps, but do not change the profile of the PES.

### 3.2. Enantioselectivity

It was found experimentally that bifunctional-urea catalysts could catalyze the nitroolefin Michael reaction with high enantioselectivity; however, the reason for the high enantioselectivity was not clarified.<sup>8</sup> To understand the origin of the enantioselectivity, the catalyzed Michael reaction of  $\beta$ -nitrostyrene and malonate was investigated.

We found that the Michael reaction of  $\beta$ -nitrostyrene has the same mechanism with the reaction of the nitroethylene. **Figure 3** shows the optimized geometries of the main TSs involved in two reaction pathways. We denote these TSs as **Ph-TS**<sub>2a-3a</sub>, **Ph-TS**<sub>2b-3b</sub>, **Ph-TS**<sub>4a-6a</sub> and **Ph-TS**<sub>4b-6b</sub>, which correspond to **TS**<sub>2a-3a</sub>, **TS**<sub>2b-3b</sub>, **TS**<sub>4a-6a</sub>, and **TS**<sub>4b-6b</sub> in the reaction of nitroethylene and malonate, respectively. The calculated results indicate that the energies of **Ph-TS**<sub>2a-3a</sub> and **Ph-TS**<sub>2b-3b</sub> are very similar, since the phenyl group of the two transition states points away from the chiral scaf-

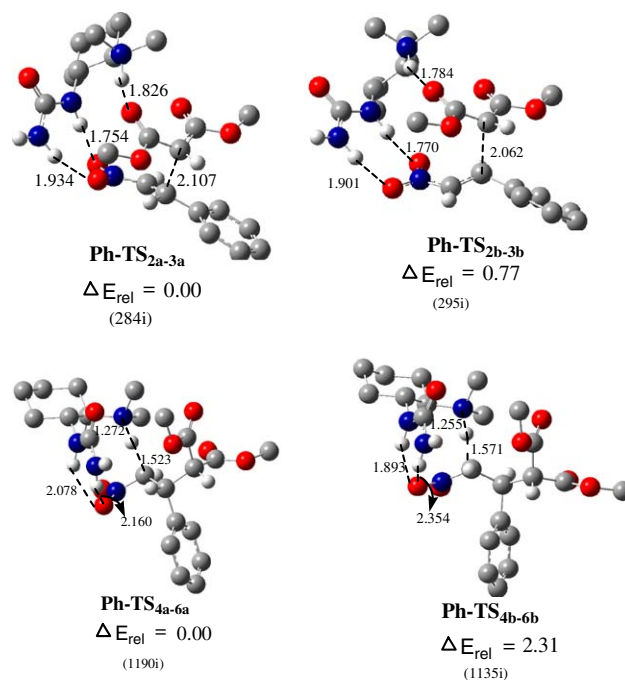


**Figure 3.** Optimized geometries of the main transition states for two reaction pathways of the reaction of  $\beta$ -nitrostyrene and malonate. The hydrogen atoms on the rings and methyl groups are omitted for clarity.

fold and does not contribute to steric repulsion. The barrier for Michael addition of pathway **B** is only 0.77 kcal mol<sup>-1</sup> higher than that of pathway **A**. However, the energy of transition state **Ph-TS**<sub>4b-6b</sub> is higher than **Ph-TS**<sub>4a-6a</sub> due to the larger energetic cost in distorting the molecular geometry to accommodate to proton transfer, and **Ph-TS**<sub>4b-6b</sub> is higher than 2.31 kcal mol<sup>-1</sup> in energy than **Ph-TS**<sub>4a-6a</sub>. The energetically favorable **Ph-TS**<sub>2a-3a</sub> and **Ph-TS**<sub>4a-6a</sub> leads to the (*R*)-product. Thus our calculated results explain the enantioselectivity observed from the experiment.

Finally, the roles of the two functional groups of the urea derivatives were reconsidered. Our calculated results show that the amino group plays a key role for the initial activation of the malonate by deprotonation, while the formation of enolate specie makes the CH group of malonate more nucleophilic. Simultaneously, the amino group and urea moiety can stabilize the stable points on the PES by hydrogen-bond interactions. In addition, our calculated results indicate that the amino group has a slight effect on the carbon-carbon bond formation. These results explain the effects of the tertiary amine functionality on the catalyzed Michael reactions.

### 4. Conclusions

A general profile of the Michael reaction catalyzed by the bifunctional-urea catalyst has emerged clearly via the DFT calculations on the prototype reaction between the malonate and nitroolefins. Four reaction channels, corresponding to the approach modes of the nitroolefins to the chiral scaffold and the second proton transfer processes,



have been characterized in detail. It was found that the enantioselectivity of the catalyzed Michael reaction is controlled by the C–C bond-formation step, while the rate determining step is the proton transfer from the amino group of the catalyst to the  $\alpha$ -carbon of nitronate. Our calculated results confirm that the amino group has a significant effect on the reaction rate, but only a slight effect on the enantioselectivity. The present DFT study explains well the experimental finding and provides the details of the reaction mechanisms.

### Acknowledgments

The work described in this paper was supported by the National Natural Science Foundation of China (No. 20473047 and 20503014) and the Major State Basic Research Development Programs (No. 2004CB719902). We thank the High Performance Computational Center of Shandong University for computer resources.

### References

1. Dalko, P. *Angew. Chem., Int. Ed.* **2001**, *40*, 3726.
2. Dalko, P.; Moisan, L. *Angew. Chem., Int. Ed.* **2004**, *43*, 5138.
3. Miller, S. *Tetrahedron* **2002**, *58*, 2481.
4. Seayad, J.; List, B. *Org. Biomol. Chem.* **2005**, *3*, 719.
5. Hayashi, Y. *J. Synth. Org. Chem. (Jpn.)* **2005**, *63*, 464.
6. Wen, Y. H.; Huang, X.; Huang, J. L.; Xiong, Y.; Qin, B.; Feng, X. M. *Synlett* **2005**, *16*, 2445.
7. Sohtome, Y.; Hashimoto, Y.; Nagasawaa, K. *Adv. Synth. Catal.* **2005**, *347*, 1643.
8. (a) Okino, T.; Hoashi, Y.; Furukawa, T.; Xu, X.; Takemoto, Y. *J. Am. Chem. Soc.* **2005**, *127*, 119; (b) Okino, T.; Hoashi, Y.; Furukawa, T.; Takemoto, Y. *J. Am. Chem. Soc.* **2003**, *125*, 12672.
9. (a) Taylor, Mark S.; Jacobsen, Eric N. *J. Am. Chem. Soc.* **2004**, *126*, 10558; (b) Fuerst, D. E.; Jacobsen, E. N. *J. Am. Chem. Soc.* **2005**, *127*, 8964; (c) Vachal, P.; Jacobsen, E. N. *J. Am. Chem. Soc.* **2004**, *124*, 10012; (d) Dove, A. P.; Pratt, R. C.; Lohmeijer, B. G.; Waymouth, R. M.; Hedrick, A. P. *J. Am. Chem. Soc.* **2005**, *127*, 13798; (e) Matsui, K.; Takizawa, S.; Sasai, H. *J. Am. Chem. Soc.* **2005**, *127*, 3680.
10. Zhu, Y.; Drueckhammer, D. G. *J. Org. Chem.* **2005**, *70*, 7755.
11. Berner, O. M.; Tedeschi, L.; Enders, D. *Eur. J. Org. Chem.* **2002**, 1877.
12. (a) Enders, D.; Seki, A. *Synlett* **2002**, 26; (b) Andrey, O.; Alexakis, A.; Bernardinelli, G. *Org. Lett.* **2003**, *5*, 2559; (c) Ishii, T.; Fujioka, S.; Sekiguchi, Y.; Kotsuki, H. *J. Am. Chem. Soc.* **2004**, *126*, 9558.
13. (a) Becke, A. D. *J. Chem. Phys.* **1993**, *98*, 1372; (b) Lee, C.; Yang, W.; Parr, R. G. *Phys. Rev. B* **1988**, *37*, 785.
14. Hariharan, P. C.; Pople, J. A. *Theor. Chim. Acta* **1973**, *28*, 213.
15. Frisch, M. J.; Trucks, G. W.; Schlegel, H. B.; Scuseria, G. E.; Robb, M. A.; Cheeseman, J. R.; Montgomery, J. A., Jr.; Vreven, T.; Kudin, K. N.; Burant, J. C.; Millam, J. M.; Iyengar, S. S.; Tomasi, J.; Barone, V.; Mennucci, B.; Cossi, M.; Scalmani, G.; Rega, N.; Petersson, G. A.; Nakatsuji, H.; Hada, M.; Ehara, M.; Toyota, K.; Fukuda, R.; Hasegawa, J.; Ishida, M.; Nakajima, T.; Honda, Y.; Kitao, O.; Nakai, H.; Klene, M.; Li, X.; Knox, J. E.; Hratchian, H. P.; Cross, J. B.; Adamo, C.; Jaramillo, J.; Gomperts, R.; Stratmann, R. E.; Yazyev, O.; Austin, A. J.; Cammi, R.; Pomelli, C.; Ochterski, J. W.; Ayala, P. Y.; Morokuma, K.; Voth, G. A.; Salvador, P.; Dannenberg, J. J.; Zakrzewski, V. G.; Dapprich, S.; Daniels, A. D.; Strain, M. C.; Farkas, O.; Malick, D. K.; Rabuck, A. D.; Raghavachari, K.; Foresman, J. B.; Ortiz, J. V.; Cui, Q.; Baboul, A. G.; Clifford, S.; Cioslowski, J.; Stefanov, B. B.; Liu, G.; Liashenko, A.; Piskorz, P.; Komaromi, I.; Martin, R. L.; Fox, D. J.; Keith, T.; Al-Laham, M. A.; Peng, C. Y.; Nanayakkara, A.; Challacombe, M.; Gill, P. M. W.; Johnson, B.; Chen, W.; Wong, M. W.; Gonzalez, C.; Pople, J. A. *Gaussian 03*, Revision B05; Gaussian, Inc.: Pittsburgh PA, 2003.
16. Boys, S. F.; Bernardi, F. *Mol. Phys.* **1970**, *19*, 553.